

Steady-State and Transient Neutronic and Thermal-hydraulic Analysis of ETDR using the FAST code system

Sandro Pelloni, Evaldas Bubelis and Paul Coddington

Laboratory for Reactor Physics and Systems Behaviour, Paul Scherrer Institute
CH-5232 Villigen PSI, Switzerland

Tel: +41 56 310 2075 , Fax: +41 56 310 2327 , Email: Sandro.Pelloni@psi.ch

Abstract – *This paper presents a consistent neutronic and thermal-hydraulic analysis of the Experimental Technology Demonstration Reactor (ETDR) start-up core with MOX fuel pins in stainless steel cladding. For the deterministic neutronic investigations this analysis is complementary to an earlier study, where the parameters have been recalculated to assess the methods sensitivity, i.e. the different model and ERANOS options. While a different approach in the burn-up calculation, in which the critical insertion position of the bank of control rod subassemblies, CSD, is explicitly accounted for has been performed and compared to the usual methodology with control rods out. In the thermal-hydraulic investigations performed using the TRAC/AAA code, steady-state calculations were performed in which the power density taken from the neutronic analysis corresponded to various reactor conditions evaluated with these methodologies. The maximum values of the fuel and cladding temperatures in the hottest subassembly as well as the coolant outlet temperatures were compared for different reactor core states. In addition, based on the steady-state parameters, an unprotected (without reactor scram) Loss-Of-Flow (LOF) transient was analyzed and the transient behaviour compared for the different cases. In particular, it is found that the expansion of the reactor core is of similar importance as the Doppler effect and it should be considered in the ETDR accident analysis. Taking this fact into account, it may be possible to protect against a LOF transient without scram particularly if the blowers of the Decay Heat Removal system (DHR) are used.*

I. INTRODUCTION

The neutronic and thermal-hydraulic investigations, presented in this paper were performed to evaluate the characteristics of the recent ETDR start-up core design, which has MOX fuel contained within stainless steel clad (see Fig. 1)¹.

The calculations presented provide a combined thermal-hydraulic and neutronic analysis and assess the result of modelling uncertainties (e.g. core axial and radial power distributions) on the steady-state core temperatures for the most recent ETDR core. In addition a representative (loss-of-flow) transient without scram was performed to evaluate the impact of the modelling uncertainties (core axial and radial power distributions) and uncertainties in the kinetic and reactivity parameters on the natural (unperturbed) response of the core. A major conclusion from the analysis is that the uncertainties in the neutronic parameters have only a minor impact on the course of the transient, while because ETDR is a high leakage core the

reactivity feedback due to core expansion has a major impact.

The neutronics analysis was conducted with ERANOS-2.0²⁻⁴, particularly the embedded cell code ECCO and the 3D nodal transport-theory program VARIANT⁴. The following parameters were determined as a function of burn-up: the multiplication factor, k_{eff} , the reactivity coefficients, including fuel Doppler, coolant void depressurization, as well as axial and radial core expansion, the worth of the shutdown subassembly, DSD, and the worth of the control rod bank, CSD, power distributions (assembly-wise and axially). Based upon these parameters the thermal-hydraulics study was carried out in a consistent manner using the code TRAC/AAA⁵, which is part of the FAST code system⁶. Additionally the kinetic parameters needed in point kinetic calculations were also calculated, The influence of gagging for all these thermal-hydraulic channels was investigated in order to obtain a uniform exit coolant temperature. Core steady-

state conditions were determined first, in which the power density corresponded to that from the following:

1. "Beginning Of Cycle" (BOC) conditions, the control rods being all in their parking position (approach "cr out"),
2. BOC conditions, the CSD subassembly bank being inserted to its critical position ($k_{eff}=1$) and the shutdown subassembly; DSD, being in its parking position (approach "cr in"), and
3. the same, but for "End Of Cycle" (EOC) conditions, corresponding to 341 effective full power days.

The maximum values of the fuel and cladding temperatures in the hottest subassembly as well as the coolant outlet temperatures were compared for the different reactor core states. In addition, based on the steady-state parameters, an unprotected Loss-Of-Flow (LOF) transient, i.e. without reactor scram, was primarily analyzed with point kinetics, spatial effects being found small in the current investigations, and the transient behaviour compared for the different cases.

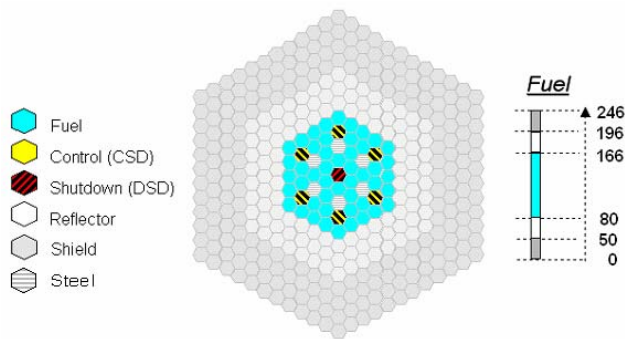


Fig. 1. ETDR start-up configuration: Cross-sectional view and dimensions (cm) in the axial direction

In particular, it is found that the (axial) expansion of the reactor core is of similar importance as the Doppler effect and it should be considered in the ETDR accident analysis, while the influence of the specific power distribution and neutronic parameters on the overall transient behaviour is negligible. Taking these facts into account, it may be possible to protect against a LOF transient without scram particularly if the blowers of the Decay Heat Removal system (DHR) are used.

The neutronics analysis is presented in Section II, the thermal-hydraulics analysis including the transient study in Section III, while Section IV is dedicated to the conclusions.

II. NEUTRONICS ANALYSIS

Table I shows that transport-theory is required for analyzing the ETDR startup core, which is a small, high-leakage system. The large transport-theory effect expressed

relative to a "pure" diffusion-theory result, which was obtained without the use of directional diffusion coefficients, amounts to ~ 2800 pcm^a (corresponding to 8 \$, see Table VI) in the case of operating conditions, and to an even larger value (~ 9 \$) if the reactor is cold. Opposite to the experience gained in analyzing larger systems, the approximated transport-theory, which usually allows to take into account a large fraction of the transport effect by reduced computing time⁴, is also seen to significantly underestimate the k_{eff} -value with respect to the exact transport-theory value, i.e. by ~ 4 \$. Therefore, P₁ transport-theory was systematically used in all further calculations.

Table II summarizes the Doppler constant, which is expressed as $\Delta\rho/\ln(T_f/T_i)$, where $\Delta\rho$ is the reactivity variation due to a temperature change from T_i to T_f , i.e. $T_i=880^\circ\text{C}$ and $T_f=180^\circ\text{C}$ in this study.

TABLE I
 k_{eff} (BOC) obtained with different methods

Reactor conditions	P ₁ -transport	P ₁ -transport approximate	Diffusion
"cold"	1.03906	1.02588	1.00977
"operating"	1.02869	1.01443	0.99729

TABLE II
 Doppler constant

pcm	BOC	EOC
"cr out"	-284	-289
"cr in"	-264	-283

The magnitude of the Doppler constant increases at EOC, which can primarily be attributed to Pu burning (see Table VIII). With the "cr in" approach, the difference between the EOC and BOC value becomes even larger, mainly as a result of the additional control rod withdrawal.

Table III gives the full depressurization reactivity coefficient. The effect of considering the CSD subassembly bank is qualitatively similar to the Doppler constant in the sense that the increase of the coefficient is of similar magnitude.

TABLE III
 Full depressurization reactivity coefficient

pcm	BOC	EOC
"cr out"	107	115
"cr in"	117	135

The axial and radial core expansion coefficients, viz. $\alpha_a = -3.14693 \cdot 10^{-6}$ and $\alpha_r = -1.03275 \cdot 10^{-5} \text{K}^{-1}$, were

^a 1 pcm = 10^{-5} .

determined from dedicated ERANOS calculations in such a way that a change in core reactivity due to the expansion of the core can be approximated with a bilinear expression of the form $\alpha_a \Delta T_f + \alpha_r \Delta T_s$, where ΔT_f is the change in the average fuel temperature and ΔT_s is the change in the temperature of the core support structure.

Table IV displays the control rod worth. For the DSD subassembly, by comparing the "cr in" approach with the "cr out" approach, the former leads for BOC conditions, to a larger value, since the flux level near the centre is enhanced through the partially inserted CSD subassembly bank located in the outer part of the core region, and this effect dominates against spectrum hardening.

TABLE IV

DSD subassembly worth and rest worth of the CSD bank

pcm	DSD (BOC)	DSD (EOC)	CSD (BOC)	CSD (EOC)
"cr out"	5427	5558	12924	15947
"cr in"	5580	5132		

At EOC, the situation is reversed, in which case the standard approach "cr out" is not conservative. The larger EOC value of the CSD bank (by ~25%) ("cr out") can primarily be attributed to control rod withdrawal.

Table V shows the maximum power density.

TABLE V

Maximum power density

Wcm ⁻³	BOC	EOC
"cr in"	169.45	163.79
"cr out"	179.94	164.44

At BOC, the "cr out" value is 6% smaller than the corresponding "cr in" value. This discrepancy is less pronounced for EOC conditions as a result of control rod withdrawal when the approach "cr in" is taken. In addition power peaking is less pronounced, as a result of Pu burning. It is also found that for BOC conditions, the energy deposited in the core region is 98%, while 1.5% is deposited in the reflector and the remaining 0.5% in the shield region, these values being almost methods independent. At EOC, the corresponding split is 97%, 1.5%, and 1.5%.

Fig. 2 shows the axial power density profile in the hottest "pin" of the hottest subassembly (i.e. near the core center). In this figure the x -coordinate refers to the height with the zero level being set at the bottom of the lower axial reflector. Compared are the "cr in" with the "cr out" calculations for BOC conditions, with the "cr in" calculation showing a perturbed cosine shape. The

maximum value of the "cr in" power density is ~10% larger and is moved towards the lower part of the active length, due to control rod insertion. As expected, a jump in the power density corresponding to the insertion position of the CSD bank is also seen.

As regards the power distribution in the radial direction, it is found that also in this case the maximum "cr in" value is larger than the corresponding "cr out" value. Such that for the "cr in" calculation the maximum subassembly power varies between 1.35 and 0.78 MW for BOC conditions, and between 1.28 and 0.80 MW for EOC conditions.

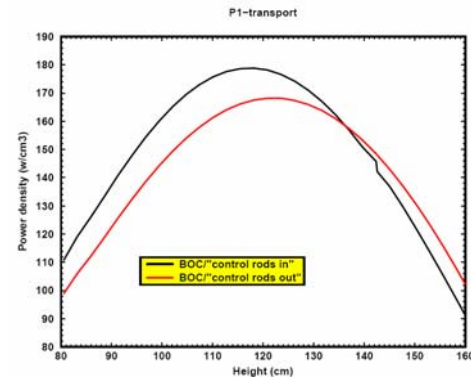


Fig. 2. Axial power distribution (ETDR start-up core)

Table VI shows the kinetic parameters. In this case, no strong sensitivity is exhibited with respect to the method or to the burnup.

TABLE VI

Kinetic parameters

Parameter	BOC		EOC	
	"cr in"	"cr out"	"cr in"	"cr out"
β_{eff} (pcm)	338	337	345	345
Λ (μ s)	0.40	0.38	0.41	0.40

Table VII summarizes the breeding gain. The negative values, which are methods independent, indicate that the ETDR start-up core is a burner.

TABLE VII

Breeding gain

	BOC	EOC
"cr out"	-1.107	-0.728
"cr in"	-1.091	-0.727

In a global sense, the neutronic analysis shows that the approach "cr in" increases the power peaking factor and makes the reactivity coefficients less favourable. This is

particularly so for BOC conditions since the ETDR-startup core is a burner. Therefore, the usual approach ("cr out") appears not conservative, for this reactor core.

III. THERMAL-HYDRAULICS ANALYSIS

The thermal-hydraulics analysis was performed using TRAC/AAA⁵, which is part of the FAST code system⁶ for the transient analysis of advanced reactors.

The general nodalization scheme used for the ETDR start-up configuration is shown in Fig. 3. The reactor pressure vessel is modelled using a 3D vessel component. The reactor core is represented by 60 one-dimensional pipe elements (components 1002, 1003, etc.) representing the channels (see Table VIII). Associated with each channel are corresponding heat structures (components 141, 142, etc.) describing the structural elements of the subassemblies. The 3D vessel component has designated zones for the lower and upper plenum, as well as for the downcomer, and has outer connections to the primary and decay heat removal (DHR) cooling circuits. During normal operation only the primary cooling circuit functions, while the DHR circuit is closed by a valve (component 2010). The main cross-duct pipe between the vessel and the main heat exchanger is modelled as a part of pipe component 1060.

The primary cooling circuit consists of the main heat exchanger, the main blower (component 12) and the primary circuit isolation valve (component 1201).

Fill component 230, pipe component 210 and break component 240 represent the secondary side of the main heat exchanger, which is water cooled. The main blower is modelled by a pump component, using the main blower head and torque homologous curves.

The primary heat exchanger is a "tube and shell" heat exchanger with the helium flowing on the shell side. The shell side flow path is directed across the tubes in a "more-or-less" cross flow pattern and therefore the primary (helium) side heat transfer correlation of Dittus-Boelter ($Nu = 0.023Re^{0.8}Pr^{0.33}$) was replaced by the Incropera cross-flow correlation ($Nu = 0.55Re^{0.56}Pr^{0.33}$)⁷. This was found to produce more accurate results without any need for artificial "fouling" or area correction factors. Valve component 1250 and break component 1255 are reserved for the calculation of Loss of Coolant Accidents (LOCA transients).

Each of the three DHR loops consists of the He and H₂O circuits (components 2011, 2004, 2012, 2008, 2010, and 2210, 2200, 2250, 2243, 2220, respectively), as well as the H₂O pool (components 2259, 2260, 2261). The two heat exchangers, He-H₂O and H₂O-H₂O were modelled with components 2004, 2210, heat structure component 9240, and components 2250, 2260, heat structure component 9000, respectively.

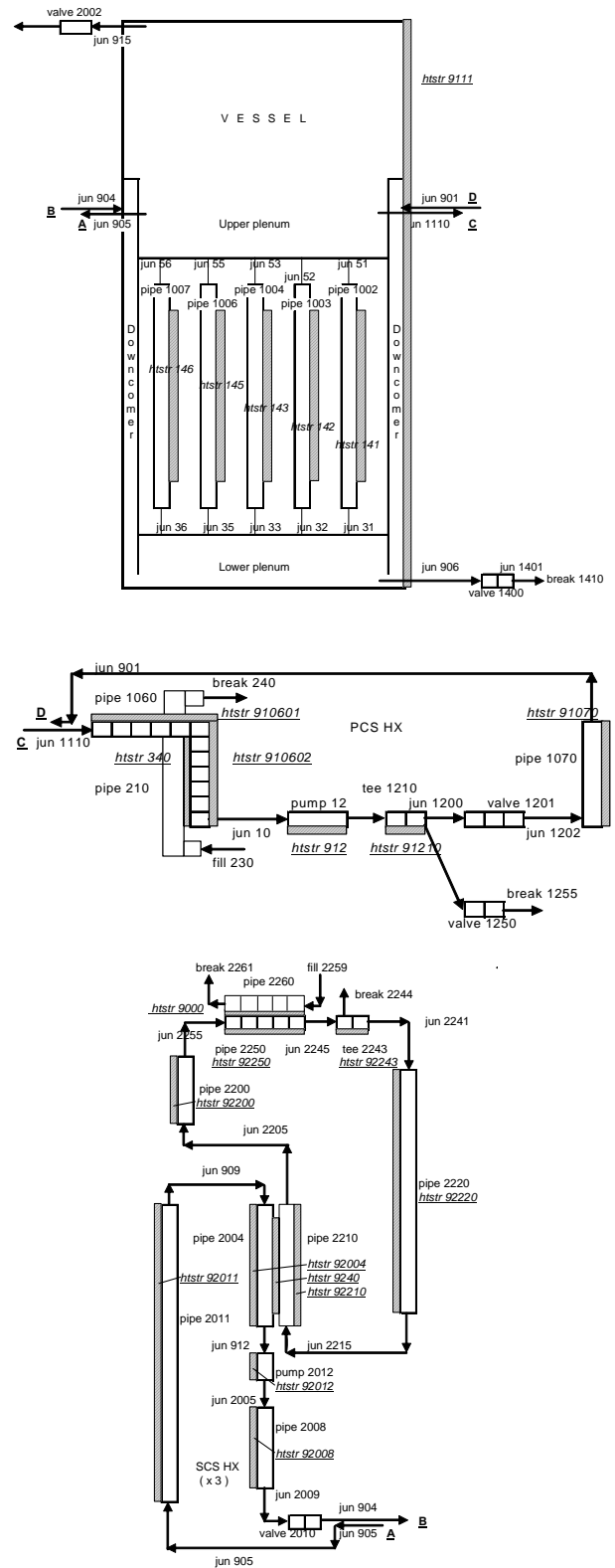


Fig.3. TRAC/AAA nodalization. From the top to the bottom: Pressure vessel, primary circuit and secondary cooling system including one loop of the Decay Heat Removal (DHR) system.

The secondary side of the H₂O-H₂O heat exchanger serves as a boundary condition for the heat transfer from the secondary to the tertiary cooling circuit of the DHR system. The water temperature in the DHR water pool is assumed to be 90°C and so serves as an initial and boundary temperature condition for the whole of the DHR system. Heat structure components 92011, 92004, 92012, 92008, 92210, 92200, 92250, 92243 and 92220 represent the metal of the secondary circuit piping which is important when modelling transients.

TABLE VIII

Specification of the TRAC/AAA model of the ETDR

48 fuel assemblies	48 TRAC channels (pipe comp)
6 Stainless steel assemblies	6 TRAC channels (pipe comp)
1 DSD	1 TRAC channels (pipe comp)
6 CSD	1 TRAC channel (pipe comp)
Radial reflector	2 TRAC channels (pipe comp)
Radial shield	2 TRAC channels (pipe comp)
Total number of TRAC channels	60

III.A. Steady-state conditions

We recall that in the first set of neutronic calculations, the power distribution corresponds to BOC conditions, approach "cr out" (see Section I). For the corresponding thermal-hydraulic calculations the TRAC channels were gagged in such a way as to obtain the same coolant temperature at the outlet of each fuel channel.

The ETDR steady-state primary system conditions for the gagged core are: a main blower flow rate of 32.0 kg/s; a total loop pressure drop of 0.991 bar and a core pressure drop of 0.532 bar; with a core (He) inlet temperature of 260°C and a core (He) outlet temperature of 560°C corresponding to a core temperature rise of 300°C. The clad and fuel maximum temperatures of the hottest subassembly are found to be 640 and 1153°C, respectively.

For the second calculation, the power distribution corresponded to BOC conditions, "cr in", while the thermal-hydraulic channel gagging scheme was taken from the first "cr out" analysis. Compared to the "cr out" case, the maximum channel power is ~3% larger and the axial peaking factor is also somewhat larger. In the hottest subassembly, these two effects result in increased clad and fuel temperatures of 645 and 1193°C, respectively. The lower than expected increase in the cladding temperature in particular, comes from the fact that the peak power location is now lower in the core (see Fig. 2) i.e. at a lower coolant temperature.

In the third calculation, the power distribution corresponded to EOC "cr in" conditions. Again the same

thermal-hydraulic gagging scheme was used. The maximum channel power is ~5% lower than in the "cr in" BOC case and the axial power peaking factor is also smaller resulting in peak clad and fuel temperatures in the hottest channel of 633 and 1125°C, respectively. Separate from these higher values of the coolant outlet temperatures are noticed in the control rod channels because of the increase in the power deposited in these channels as the burnup increases. It is important therefore that the gagging in the non-fuel channels is based on the highest power expected in these channels. This of course means that these channels will be "over-cooled" at the beginning of the cycle. From the above it is clear that, as part of any final core design the flow distribution in the core will need to be carefully optimised and that will have to include the non-fuelled subassemblies.

The results of the steady-state calculations presented above are summarised in Table IX.

TABLE IX

Maximum clad and fuel temperatures for the cases considered

	Clad, °C	Fuel, °C
"cr out" BOC	640	1153
"cr in" BOC	645	1193
"cr in" EOC	633	1125

III.B. LOF transient without reactor scram

In order to examine the influence of the different parameters obtained from the steady-state neutronic and thermal-hydraulic analyses for the three configurations - "cr out" BOC, "cr in" BOC and "cr in" EOC, on ETDR transients a representative unprotected LOF transient was investigated. The parameters that may influence such a transient include: the radial and axial power distribution, the kinetics parameters and the reactivity coefficients.

In order to examine in detail the impact of the different parameters, two analyses were performed; the first in which only the Doppler and coolant density reactivity feedbacks were considered. This calculation was performed for all three core configurations. A second analysis in which all reactivity feedbacks were included was performed for "cr in" BOC conditions.

The sequence of events characterizing this transient are the same as during the protected LOF transient⁸, except for the reactor scram when the pump speed reaches 90 % of the nominal value. For this transient the power was calculated using point kinetics with the various parameters such as Doppler constant (see Table II), full depressurization reactivity coefficient (see Table III), core expansion coefficients (see Section II), delayed neutron fraction and neutron generation time (see Table VI) taken from the reactor state simulated, i.e. BOC, approach "cr out", BOC, "cr in", and EOC, "cr in" (see Section II). As

stated above two sets of calculations were performed: The first, in which only the Doppler and coolant density feedbacks were considered, and the second set in which the core axial and radial expansion feedbacks were added to investigate the influence of the core expansions on the transient.

Following the sequence of events, the main blower was tripped at time $t = 10$ s. But when the pump speed reached 90% of the nominal value the reactor scram was not initiated. The transient was simulated, until the fuel clad temperature reached 1320 °C (it is the limiting value for the fuel clad temperature internally for TRAC/AAA). As can be seen from Figs. 4-6, in which expansion effects were not considered, the maximal fuel clad temperature is reached on 44, 40 and 46 s after the main blower trip, respectively for the three different core states.

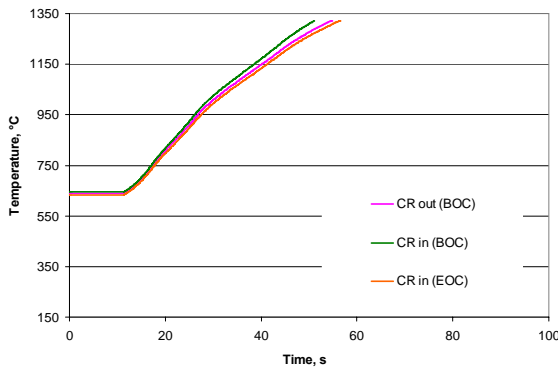


Fig.4. Maximum clad temperature in the hot channel

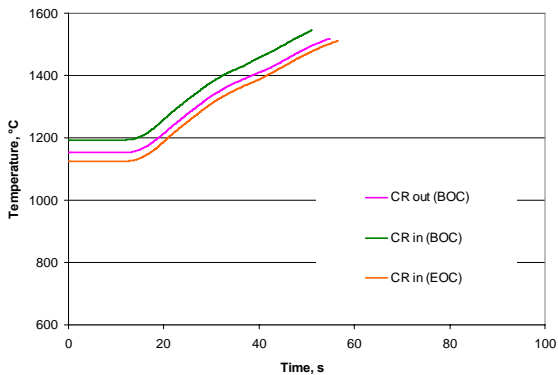


Fig.5. Maximum fuel temperature in the hot channel

After ~ 2 s, the blower speed is found to reach ~ 90 % of the nominal value. As the reactor power remains high while the total core flow rate diminishes, the fuel, clad and coolant temperatures in the core start to increase (see Figs. 4-5). The pressure at the top of the vessel increases following the increase in the average coolant temperature. Because of the decrease in the helium flow rate in the main circuit, the increase in the average coolant temperature and the heat transferred to the main heat exchanger the coolant temperature at the core inlet decreases slightly. As the fuel

temperature increases the Doppler feedback begins to reduce the reactor power (see Fig. 6) by inserting negative reactivity. This effect helps to reduce the rate of increase in the fuel and clad temperatures. But as the helium flow rate through the core is found to diminish faster than the total reactor power, the fuel and clad temperatures continue to rise. This process continues until ~ 45 s, i.e. until the moment when the fuel clad temperature reaches the value of 1320 °C and the code simulation is terminated. In general, no major discrepancy is seen between the three reactor states, viz. BOC conditions, approach "cr out", BOC, "cr in", and EOC, "cr in".

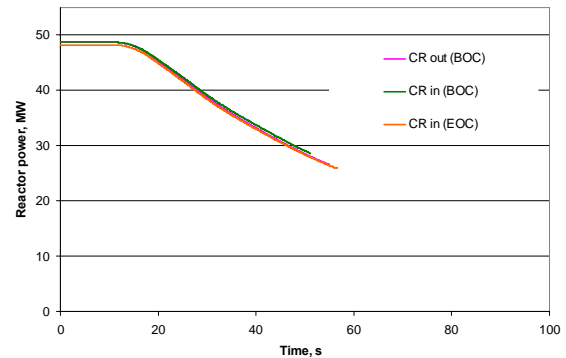


Fig.6. Reactor power

Some difference as expected is seen in the behaviour of the maximum fuel temperature in the hot channel (see Fig. 5), but this mainly comes from the different maximum linear powers and therefore the maximum steady-state fuel temperatures.

Some differences are also found in the behaviour of the maximum clad temperature and the coolant temperature at the core outlet for the three cases, but these differences are only minor and they are directly related to the different maximum fuel temperature values in these three cases. It can be concluded therefore that the ~ 10 % difference in the Doppler constant between the different core states has only a minor impact on the results of this transient.

A heat balance calculation shows that at the beginning of the transient all the heat generated by the fuel assemblies is taken away by the main heat exchanger. Starting from time $t = 10$ s, the difference between the heat generated and the heat removed by the main heat exchanger goes to heating the Helium. All the other heat balance components are small and are not significant during the unprotected LOF transient.

The results of the second calculation, in which the core axial and radial expansion feedbacks were added to investigate core expansions influence on the transient, can be seen in Figs. 7-9. The new transient calculation, corresponding to BOC conditions, "cr out" (called "CR out (BOC) with exp."), continued for 186 versus 44 s for the previous, before the calculation stopped upon reaching the

fuel clad temperature value of 1320 °C. This means that expansion reactivity feedbacks, axial expansion being found largely the main effect, delayed the time until the moment when the fuel clad temperature reached the value of 1320 °C, and are of similar importance to the Doppler effect for this reactor core. Although the power decreases more significantly, the fuel, clad and coolant temperatures in the reactor core still increase, but due to the core expansion reactivity feedbacks the temperature increase rate is smaller than for the case in which the expansion feedback was not considered. Following the temperature increase in the core region, the pressure at the top of the reactor vessel also increases, but again due to the lower power the pressure increase is smaller and the pressure stabilizes after ~100 s. Because of the decrease in the helium flow rate and due to the heat removed by the main heat exchanger, the coolant temperature at the core inlet decreases and stabilizes after ~100 s of the transient.

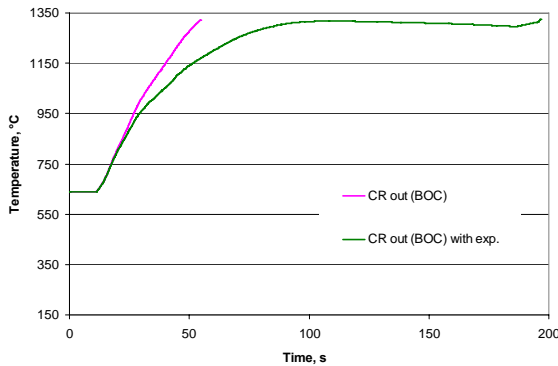


Fig.7. Maximum clad temperature in the hot channel

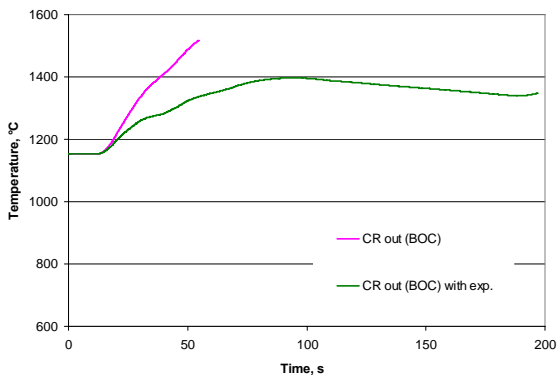


Fig.8. Maximum fuel temperature in the hot channel

As the fuel temperature increases, the Doppler as well as the axial core expansion feedbacks reduce the reactor power (see Fig. 9) by inserting negative reactivity (see Fig. 10). If the reactivity feedbacks coming from the core expansion are accounted for, the reactor power decreases at a larger rate due to the core axial expansion and in this case the core power is reduced from 50 to ~8 MW after ~170 s (see Fig. 9). As is shown in Fig. 10 there are

approximately equal contributions to the reactivity feedback coming from the Doppler and from the core expansion. These two effects help to reduce the fuel temperature increase.

After about 100s a "quasi" equilibrium is reached in which the core temperatures (fuel, clad and coolant) are constant and even reduce slowly. Therefore during this period the core power, which is typically ~ 10 % of the nominal value, is removed by the main heat exchanger in spite of the reduction in the main coolant flow rate.

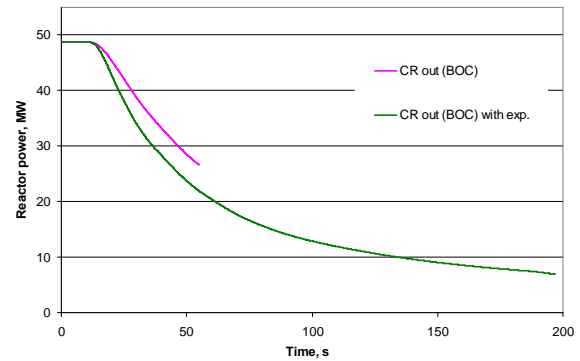


Fig.9. Reactor power

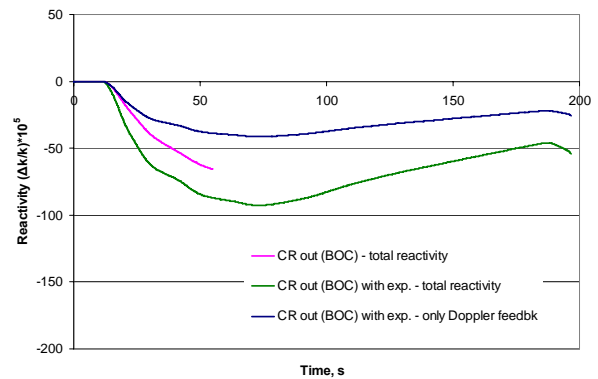


Fig.10. Core reactivity

After ~174 s from the start of the transient, the blower speed reaches 5% of its nominal value and the main circuit is isolated over a period of 10 s. At the same time the DHR circuit is opened. Due to the fact that the natural circulation flow of helium through the DHR loop is established only after about 50 to 100 s, the temporary reduction of the helium flow through the core after switching from the main cooling circuit to the DHR cooling circuit, results in the rapid increase in the core temperatures (see Figs. 7-8). This leads to the fuel clad temperature increase up to the value of 1320 °C at ~ 186 s and at this time the code simulation is terminated.

The general conclusions from this simulation are:

- that the reactivity feedback from the axial and radial expansions of the reactor core are of equal importance to the Doppler and should be taken into account in the ETDR accident analysis;

- it may be possible to protect against a LOF transient without scram particularly if the DHR blowers are used.

IV. CONCLUSIONS

As a complement to an earlier study, the neutronic parameters of the ETDR start-up configuration have been recalculated with ERANOS-2.0 using different options. In particular, diffusion-theory has been compared with P_1 transport-theory, and the influence on the reactor parameters of the actual control rod position used to make the reactor critical has been investigated. The calculations were performed for a first batch of 341 effective full power days. More specifically, within a first approach called "cr out", the standard method was used, in which the control subassemblies, i.e. the CSD subassembly bank and the shutdown subassembly DSD, are not inserted during the entire irradiation period. For the second more rigorous approach, viz. "cr in", the DSD subassembly is not inserted, whereas the CSD subassembly bank, depending on the burn-up of the core, is partially inserted such as to maintain the system critical. It has been found that:

There is a strong methods sensitivity, in particular the transport-theory effect on the multiplication factor k_{eff} is as much as 3000 pcm.

The "cr in" approach (in conjunction with P_1 transport-theory) often leads to different results when compared to the "cr out" methodology.

Also, the "cr out" result do not always appear conservative from the safety viewpoint (lower peak power, better reactivity coefficients).

Consistent with these investigations a thermal-hydraulic analysis was carried out using the TRAC/AAA code. In particular, the power distribution used in these calculations corresponded to three representative core states with respect to the (static) neutronic calculations, namely: 1) BOC conditions, "cr out", 2) BOC, "cr in", and 3) EOC, "cr in". A fuel channel gagging scheme was designed using the power distribution from the "cr out" BOC conditions to keep the same exit coolant temperature.

In the steady-state calculations, the maximum values of the fuel and cladding temperatures in the hottest subassembly were compared, as well as the coolant outlet temperatures.

Main points are:

More conservative parameters (higher peaking factors leading to higher temperatures) are obtained in the case when the power distribution corresponds to BOC conditions, "cr in";

The larger power deposited in the non-fuel channels associated with the power distribution for EOC conditions, "cr in", limits the coolant flow rate in these channels. Therefore, the coolant outlet temperatures, which vary in the different channels, are much larger, in this case.

Gagging the non-fuel channels, based upon the EOC power distribution, is thus preferable;

To determine the influence of the different core parameters obtained for the three core configurations an unprotected LOF transient was performed. The results show a negligible influence of the specific power distribution and neutronic parameters on the overall transient behaviour;

While the reactivity feedback from the axial and radial expansions of the reactor core, axial expansion being largely the most important effect, are of similar importance to the Doppler effect for this reactor type and they should be considered in the ETDR accident analysis. Taking this into account, it may be possible to protect against a LOF transient without scram particularly if the DHR blowers are used.

NOMENCLATURE

ETDR - Experimental Technology Demonstration
Reactor
DHR - Decay Heat Removal

REFERENCES

1. C. Poette et al., "Status of the ETDR Design", Paper 7208 of the 2007 International Congress on Advances in Nuclear Power Plants - ICAPP'07.
2. J. Y. Doriath et al., "ERANOS 1: The advanced European system of codes for reactor physics calculations", *Proc. Joint Conf. on Mathematical Methods and Supercomputing in Nuclear Applications*, Karlsruhe, Germany (1993).
3. G. Rimpault et al., "The ERANOS data and code system for fast reactor neutronic analyses", *Proc. Int. Conf. on the New Frontier of Nuclear Technology: Reactor Physics, Safety and High-Performance Computing*, PHYSOR, Seoul, Korea (2002).
4. G. Palmiotti et al., "VARIANT: VARIational Anisotropic Nodal Transport for multidimensional cartesian and hexagonal geometry calculation", Technical report, ANL-95/40, Argonne National Laboratory, USA (1995).
5. J.W. Spore et al., "Accelerator Transmutation of Waste Updates for TRAC-M", Technical report, LA-UR-01-3660, Los Alamos National Lab, USA (2001).
6. K. Mikityuk et al., "FAST: An advanced code system for fast reactor transient analysis", *Annals of Nuclear Energy*, **32**, 1613 (2005).
7. W. F. G. van Rooijen, "Introductory study of the heat exchanger design and application to a conceptual design of a primary heat exchanger for ETDR", Technical report, CEA/DEN/CAD/DER/SESI/LCSI/NT DO6, CEA-Cadarache, France (2005).
8. E. Bubelis et al., "A GFR benchmark comparison of transient analysis codes based on the ETDR concept", Paper 7340 of the 2007 International Congress on Advances in Nuclear Power Plants - ICAPP'07.